Accepted Manuscript

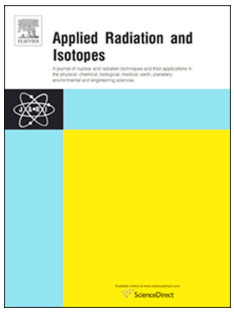

Raman spectroscopy as a tool to evaluate oxygen effects on the response of polymer gel dosimetry

D. Chacón, J. Vedelago, M.C. Strumia, M. Valente, F. Mattea

PII: S0969-8043(19)30031-4

DOI: https://doi.org/10.1016/j.apradiso.2019.05.006

Reference: ARI 8720

To appear in: *Applied Radiation and Isotopes*

Received Date: 9 January 2019

Revised Date: 4 May 2019

Accepted Date: 6 May 2019

Please cite this article as: Chacón, D., Vedelago, J., Strumia, M.C., Valente, M., Mattea, F., Raman spectroscopy as a tool to evaluate oxygen effects on the response of polymer gel dosimetry, *Applied Radiation and Isotopes* (2019), doi: https://doi.org/10.1016/j.apradiso.2019.05.006.

Raman spectroscopy as a tool to evaluate oxygen effects on the response of polymer gel dosimetry

D. Chacón[1,2], J. Vedelago[3,1], M.C. Strumia[4,5], M. Valente[3,1,6] and F. Mattea[4,5,1*]

[1] Laboratorio de Investigación e Instrumentación en Física Aplicada a la Medicina e Imágenes por Rayos X (LIIFAMIR[x]), FAMAF, Universidad Nacional de Córdoba, M. Allende s/n, Córdoba, Argentina.
[2] Departamento de Física, Universidad Nacional, Heredia, Costa Rica.
[3] Instituto de Física Enrique Gaviola (IFEG) - CONICET, M. Allende s/n, Córdoba, Argentina.
[4] Departamento de Química Orgánica, Facultad de Ciencias Químicas, Universidad Nacional de Córdoba, CONICET, Córdoba, Argentina.
[5] Instituto de Investigación y Desarrollo en Ingeniería de Procesos y Química Aplicada (IPQA), CONICET, Córdoba, Argentina
[6] Departamento de Ciencias Físicas & Centro de Física e Ingeniería en Medicina - CFIM, Universidad de La Frontera, Francisco Salazar 1145, Temuco, Chile.

E-mail: fmattea@gmail.com, fmattea@fcq.unc.edu.ar

Abstract
Currently, advanced dosimeters like polymer gels are capable of reliable and accurate 3D dose distributions obtained from correlation with the different polymerization degrees induced by incident radiation. Samples of polymer gel dosimeters are commonly read out using magnetic resonance imaging or optical methods like visible light transmission or laser computed tomography. Alternatively, this work proposes and evaluates the implementation of Raman spectroscopy to provide direct information on the chemical changes of each monomer that polymerized, due to irradiation, for three types of polymer gel dosimeters, namely NIPAM, ITABIS and PAGAT. The aim of the present study is to provide better and complete interpretations using three different containers, adequate for integral, 2D and 3D dose mapping. Moreover, Raman spectroscopy has been used to analyze the well-known effect of oxygen inhibition on the different polymer gel dosimeters remarking the importance of avoiding air exposition during sample storage and readout. Dose-response curves for different polymer gels were obtained in terms of measurements with a calibrated ionization chamber. Additionally, dedicated Monte Carlo simulations were performed aimed at characterizing dose rate for different X-ray irradiation setups, providing also suitable information to evaluate oxygen diffusion through the sample wall. The obtained results were contrasted with optical transmission readout as well as Monte Carlo simulations attaining very good agreements for all dosimeter types.

Keywords: Raman spectroscopy, Polymer gel dosimetry, Oxygen inhibition, PAGAT, NIPAM, Itaconic acid

1. Introduction

Dosimetry plays an essential role in most clinical applications of ionizing radiation like radiotherapy or radiology, and it's the main method to provide a reliable verification of the dose delivered to a patient. There are many different types of dosimetry systems, such as ionization chambers, thermoluminescent dosimeters (TLDs), optically stimulated luminescent (OSLs), scintillators, diodes, radiochromic films, Fricke and polymer gels, and most of them are used within tissue equivalent materials (Doran, 2009). Among them, gel dosimetry has the advantage of providing, not only quantitative information on the delivered dose, but also the three-dimensional distribution of that dose. In particular, polymer gel dosimeters (PGDs) have been proposed and used because of their low post irradiation diffusion compared to other typical systems like Fricke gel dosimetry (Baldock et al., 2010). Since the initial proposal of using PGDs as dosimetry materials (Maryanski et al., 1993) and considering their advantages against Fricke gel dosimetry (Schreiner, 2004), a large number of monomers and combination of monomers have been proposed and studied (Titus et al., 2016) proving their capacity as dosimetry systems to preserve the spatial distribution of absorbed dose (De Deene et al., 2001; Ibbott et al., 1997). However, there are still concerns on the optimal composition of these materials, their stability, spatial integrity, temperature

sensitivity, dose and energy dependence, tissue equivalence, and on which is the best readout method to retrieve the proper information once irradiated. These issues have limited the applicability of PGDs for routine clinical dose verification (Sedaghat et al., 2012; Baldock et al., 2010).

PGDs contain chemical species such as monomers and crosslinking agents that react upon irradiation forming polymers or hydrogels within a gelatin matrix. Ionizing radiation induces water radiolysis forming free radicals, which interacts with the monomers and crosslinking agents giving place to the initiation step of polymerization reactions. Afterwards, the polymer radicals interact with other monomers or crosslinking agents and grow in size and complexity forming large and dense macromolecules that become insoluble in the gelatin matrix. Therefore, these macromolecules appear as solids or gels interpenetrated with the gelatin matrix of the dosimetry material. The propagation and growth step in this reaction ends when two radicals react between each other or when they react with other species like oxygen or peroxides leading to the terminations step of the polymerization reaction. This complex mechanism on how the radiation interacts with the different chemical species is sensitive to external factors, such as oxygen or temperature, therefore an exhaustive control during the manufacturing and irradiation of such systems must be carried out to ensure the reproducibility and performance of the dosimeters. It has been suggested from their first implementations that dissolved oxygen is one of the main sources of error in PGDs (Maryianski et al. 1994; Jirasek et al, 2006; Sedaghat et al., 2011). Moreover, the use of antioxidants together with the main components of a PGD has been proposed during their manufacturing since the year 2001 (Fong et al., 2001), known as normoxic polymer dosimetry. Nevertheless, large differences can be observed in scientific reports of similar materials, indicating that content of oxygen in the dosimeters represents a key variable for the reproducibility in their use. Moreover, oxygen can go through typical phantom materials where PGDs are used and still be an issue regarding to reproducibility and reliability (Jirasek et al., 2006). This effect can be minimized by using different specific materials like Barex or special glass (Deene and Vandecasteele, 2013). However, the use of 3D printed phantoms still relies on the use of common polymers that are not inherently impermeable to oxygen, for example polylactic acid, a resin based on polyvinyl butyral and VisiJet photopolymer were evaluated for 3D printing of phantoms for PAGAT dosimetry and compared to barex observing a “wall effect” associated to the diffusion of oxygen through the phantom walls (Elter et al., 2019).

Among the different readout methods to study these effects on PGDs, optical methods, MRI or ultrasound are typically used because of their availability on medical facilities or simplicity to perform (Jirasek et al., 2006; Lepage, 2006; Mesbahi et al., 2012). However, the use of more direct techniques like Raman spectroscopy could provide a precise insight on changes in the chemical structure of sample constituents and, therefore, offers a unique tool to study the polymerization taking place in the dosimeters. In that regard, Baldock et al. (Baldock et al., 1998) were the first to use Raman spectroscopy for the study of monomer consumption in irradiated polymer gel dosimeters, and since then several studies on the use of Raman spectroscopy with different polymer gel dosimetry were reported (Adenan et al., 2014; Huang et al., 2013; Jirasek, 2010; Mattea et al., 2015a; Rintoul et al., 2003), which show the potentiality of the technique to evaluate the consumption of each reactive species separately, and also to study more complex mechanisms taking place in the gels like the interaction between typical antioxidants with the monomers, gelatin or other species present in the dosimeter.

The main goal of this study is to use Raman spectroscopy to assess the effect of oxygen on the polymerization induced by the radiation on different normoxic polymer dosimetry systems, based on polyacrylamide (PAGAT), N-isopropylacrylamide (NIPAM), and itaconic acid (ITABIS), and in particular the inhibition caused by oxygen entering to the dosimeter after its manufacturing through the walls of their container or phantom. This effect, although being reported in the past, is not typically acknowledged by many authors and could represent a source of error in the analysis of dose distributions. Additionally, this study shows the benefits of using a readout technique able to account for the differences in the chemical species in the dosimeters with high spatial resolution over other typical analytical methods.

2. Materials and methods

2.1. *PGD manufacturing*

All the materials used to prepare and manufacture the dosimeters are depicted in Table 1. The PGDs were manufactured based on the method published elsewhere (Mattea et al., 2015a; Vedelago et al., 2016; Venning et al., 2005). NIPAM and PAGAT dosimeters were prepared with ultra-pure water, while ITABIS materials were prepared in an aqueous phosphate buffer solution (PBS) of 0.1 M with a pH of 7.0.

Briefly, 90 wt.% of the water used in the dosimeters was mixed with porcine skin gelatin with the aid of magnetic stirring for 10 minutes at 20 ºC and 250 rpm. Afterwards, the temperature was raised up to 45 ºC with constant stirring for at least 30 minutes, until a homogenous solution was obtained. Then, N, N'-methylenebisacrylamide (MBA) was added and the whole solution was mixed for 15 minutes at 45 ºC. Next, the temperature was lowered to 37 ºC and the monomer, namely NIPAM, AAm, or ITA was incorporated. The whole solution was mixed at 37 ºC for 30 minutes. The THPC was added together with the remaining 10 wt.% of the water at 35 ºC, and the final solution was kept at this condition for 2 minutes. Finally, polymethyl methacrylate (PMMA) cuvettes of 10 x 5 x 40 mm^3, with a wall thickness of 1 mm, were filled with the solution and stored at 4 ºC until their irradiation. Although there are studies showing that a concentration of 5 mM of THPC is enough to remove all dissolved oxygen in the dosimeters (Jirasek et al., 2006), in this study the concentration of THPC was set to 10 mM to provide additional antioxidant to consume the oxygen that could enter into the dosimeters through the wall of the container. This concentration has been previously reported (Mattea et al., 2015a, Rabaeh et al., 2017) and didn't cause any pre-irradiation polymerization on the material as suggested by Senden et al. (Senden et al., 2006), providing low optical absorbance values in the unirradiated dosimeters."

Table 1. Chemical composition of the different studied PGDs: NIPAM, PAGAT and ITABIS.

Component	Acronym	Provider and characteristics	**NIPAM[b]**	**PAGAT[b]**	**ITABIS[b]**	
Water or PBS[a]	H2O	--	87.00	89.00	90.00[a]	wt.%
Porcine skin gelatin	GEL	Gelatin 300 Bloom, purchased from FLUKA	5.00	5.00	5.10	wt.%
N, N' methylene bis acrylamide	MBA	99% purity, purchased from Sigma Aldrich ®	3.00	3.00	1.59	wt.%
N-isopropyl acrylamide	NIPAM	97% purity, purchased from Sigma Aldrich ®	5.00	--	--	wt.%
Acrylamide	AAm	99% purity, purchased from Sigma Aldrich ®	--	3.00	--	wt.%
Itaconic acid	ITA	99% purity, purchased from Sigma Aldrich ®	--	--	3.06	wt.%
Tetrakis-phosphonium chloride	THPC	80% solution in water purchased from FLUKA	10	10	10	mM

[a]In the ITABIS preparation the solvent of the dosimeter was a phosphate-based buffer solution instead of water.

[b]The errors in the reported wt. % were below 0.007 % and below 0.1 mM in the reported mM concentrations.

2.2. *Storage and pre-irradiation conditions*

Because the presence of oxygen could affect the overall performance of the PGDs, the prepared materials were stored in three different conditions. A first set was stored for 2 h at 4 ºC and then irradiated, a second set was stored for 48 h at 4 ºC in a nitrogen atmosphere and then irradiated and the last set was stored for 48 h at 4 ºC and then irradiated. Table 2 summarizes the different sets and pre-irradiation conditions of these materials.

2.3. Irradiation setup

The different sets were irradiated in an X-ray tube described elsewhere (Valente et al., 2016), with a W anode connected to a generator (Siemens Kristalloflex, Germany) with an incident beam collimated to a 50 x 50 mm^2 square geometry, using an electrical current of 44 mA, voltage of 44 kVp, a source-to-phantom distance of 800 mm and a collimator to sample distance of 10 mm. The dose range of each set of PGDs is depicted in Table 2 and was established depending on the minimum dose to obtain a signal in the PGDs. The dose rate was estimated by means of calibrated ionization chambers, namely farmer type (PTW-Freiburg 30013) and pinpoint (PTW-Freiburg 30006) as well as a specific detector for medium and low X-ray energies (0.2 cm^3 PTW-Freiburg 23344) inserted in solid water equivalent phantoms. In addition to calibration factors, cross-calibrations were previously carried out following the recommendations of IAEA TRS-398 Protocol, which are mainly described in sections 4.3.2 and 5.5 of the report (IAEA, 2000) for each detector. Cross-calibrations were performed using ^{60}Co and X-rays of 30 kVp (Aluminum half value layer of 0.37 mm) in agreement to reference conditions for the different ionization chambers. After cross-calibrations, deviations of the obtained factors were less than 2.5% in all cases. In fact, the obtained cross-calibration factors compare well with those on their respective chamber certificates. Every sample was irradiated with a "box" technique using four opposite and parallel fields.

Table 2. Pre-irradiation conditions and dose range of the different PGDs.

Set	PGD	Pre-irradiation environment	Pre-irradiation time [h]	Dose range [Gy]
N1	NIPAM	Air	2	0-16
N2	NIPAM	Nitrogen	48	0-16
N3	NIPAM	Air	48	0-16
P1	PAGAT	Air	2	0-16
P2	PAGAT	Nitrogen	48	0-16
P3	PAGAT	Air	48	0-26
I1	ITABIS	Air	2	25-100
I2	ITABIS	Nitrogen	48	25-100
I3	ITABIS	Air	48	25-100

In this study, high precision in the time lapses between the manufacturing, irradiation and analysis of the different materials was crucial to compare and justify the differences observed due to oxygen diffusion or stabilization processes. Therefore, the use of in-lab equipment for the irradiation and characterization of the materials was necessary. In addition, there are many authors proving that PGDs have a linear response in orthovoltage photon beams (Boudou et al., 2007; Gastaldo et al., 2008; Hill et al., 2005), and despite that the linear response might not be the same than in the megavoltage range it is still useful to evaluate if Raman spectroscopy is able to quantify the effect of oxygen and oxygen diffusion on the polymerization occurring during the irradiation of these PGDs.

2.4. Dose distribution simulations

The dose rate was measured at different depths with the ionization chamber in a solid water equivalent phantom at depths ranging from 2.6 mm to 6.6 mm with a 1.0 mm resolution. The measured dose rates were fitted with exponential functions and two different setups were fitted in this way. A scheme of the cuvettes and the different setups is presented in Figure 1. The dose rates obtained in the central part of the samples with the setups already described and presented in Figure 1 are (0.73 ± 0.03) Gy/min in Setup A and (1.31 ± 0.05) Gy/min in Setup B.

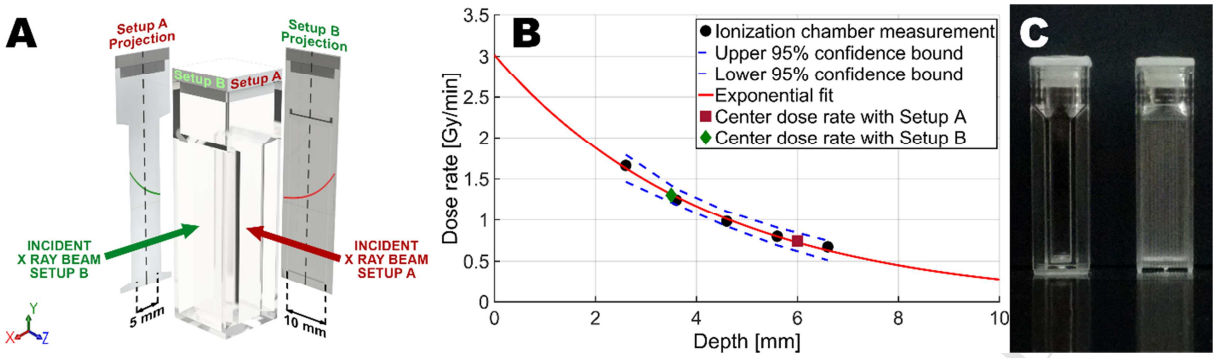

Figure 1. (A) Scheme of the different irradiation setups to simulate the dose and dose distribution within the samples. (B) Dose rate measurements and estimation for the two different irradiation setups. (C) Front and left side of the cuvettes.

The dose distribution was obtained by Monte Carlo (MC) PENELOPE simulations (Salvat et al., 2006) by using the already described irradiation geometry and an incident spectrum obtained by means of a Cd-Te XR-100 Amptek® detector (Bedford, USA) at 44 kVp. The acquired signal was properly processed by the DPPMCA software provided by the manufacturer in order to perform an energy calibration and corrections related to background, gain adjustment, absorption edges and escape peaks. The corrected spectrum was used as an input for the MC simulations to sample the photon initial energy for each experimental case. For each setup, a rectangular incident beam of 12 x 40 mm was simulated with a source to surface distance (SSD) of 800 mm, a sample of 10 x 5 x 40 mm^3 and $1x10^9$ primary showers. The simulation parameters of PENELOPE were set to default values, namely C_1=C_2=0.1 and W_{CC}=W_{CR}=5 keV. Finally, the dose distribution was normalized to the dose at the center of the sample to simplify the analysis of dose gradients.

2.5. PGD response characterization

Three different techniques were used to analyze the response of the PGDs, namely optical absorbance and transmission, magnetic resonance imaging and Raman spectroscopy**.**

2.5.1. Optical absorbance measurements

A Shimadzu® UV-1800 spectrophotometer (Japan) was used to measure the optical absorbance of every sample in this study. The wavelengths chosen for the analyses were set to have the highest sensitivity within the saturation value of the spectrophotometric method. Therefore, a wavelength of 540 nm was set for NIPAM and PAGAT dosimeters and of 430 nm for ITABIS (Mattea et al. 2015a). The absorbance was determined before and 24 h after their irradiation, which has been reported by other authors as the stabilization time required for the polymerization reactions within a PGD (Senden et al., 2006). An absorbance difference (ΔA) was defined between the optical absorbance at the optimal wavelength of the irradiated sample (A_i) and the corresponding unirradiated sample (A_0). The relative absorbance at different doses was fitted to a linear function (Equation 1), where the slope *(m)* represents the PGD sensitivity and the ΔA-intercept *(n)* represents the minimum dose to obtain a response in the PGD, otherwise known as the dose threshold of the material.

$$\Delta A = A_i - A_0 = mDose + n \quad (1)$$

2.5.2. Optical transmission measurements

In order to study the dose distribution in the samples, optical transmission maps were acquired by means of an apparatus described elsewhere (Vedelago *et al.*, 2016), which consists on a homogeneous light source and charge-coupled device (CCD) camera SXV-H5 (Starlight Xpress Ltd, Binfield, UK) coupled with an optical filter of 540 nm. In this apparatus, the CCD camera was controlled through a USB port and the transmission images were recorded in gray-level maps for further analysis. A spatial

resolution of (3.74 ± 0.01) pixels/mm and an overall reproducibility of not less than 99% can be obtained with this setup. With this method, optical transmission profiles of the irradiated cuvettes were obtained, and with the information of the unirradiated dosimeters, optical density (OD) maps and profiles were calculated by means of Equation 2.

$$OD = \alpha log\left(\frac{I_0}{I}\right) \quad (2)$$

Where α represents a calibration factor, I_0 is the intensity of the dosimeter before irradiation and I the one after being irradiated. The *OD* calculated in this way is proportional to the absorbed dose. In order to obtain optical density profiles on the dosimeters, a region of interest of 41 by 16 pixels was defined in the light transmission maps, then all values at each vertical position were averaged and the OD value was calculated. The uncertainty for each OD value was obtained by means of the propagation of uncertainty method.

2.5.3. Magnetic resonance imaging

A Siemens MAGNETOM® MRI system (Symphony Maestro Class, Germany) of 1.5 T provided with a head coil and spin-echo acquisition sequence was used to analyze the irradiated and unirradiated samples. Two echo-times (TE) were set at 124 and 194 ms, with a repetition time of 5710 ms, a bandwidth of 130 Hz, slice thickness of 1 mm and distance between slices of 1.3 mm. With this configuration, 11 signals were taken and averaged at each TE. It is worth noting that samples were scanned using the minimum required different echo-times. With this setup, the total acquisition time was 30 minutes. The image processing method presented by Y. De Deene (De Deene, 2009) was used in this study, which consists briefly on using the DICOM images and processing them to obtain the relaxation rate (R2) maps by means of the expression presented in Equation 3.

$$R2 = \frac{1}{TE_2 - TE_1} ln\left(\frac{S(TE_1)}{S(TE_2)}\right) \quad (3)$$

Where *S* represents the signal obtained at each *TE*. Also, the relative relaxation rate (ΔR2) was defined as the difference between the relaxation rate of an irradiated sample and an unirradiated sample. The MRI analysis consisted on evaluating R2 in the central region of 10 x 3 voxels in the samples, then the R2 mean value of that region and its associated uncertainty was considered as the integrated response of the readout technique.

2.5.4. Raman spectroscopy

A chemical analysis of the dosimeters was performed by Raman spectroscopy with a Labram HR Micro-Raman spectrometer (Horiba Jobin-Yvon) using a 632.8 He–Ne Laser with a 4.54 mW power. The spectra of the dosimeters were analyzed at different positions over a line in the X axis at a defined position in the Y axis and at the center of the Z axis of the cuvettes. The resolution obtained with the Micro-Raman setup was 0.1 μm in the X and Y axis and less than 5 μm defined by the pinhole used during the measurements. Within this line, 6 different spectra were collected averaging 20 repetitions with an acquisition time of 10 seconds. The spectra were processed with the software Horiba LabSpec 5.9320, applying a polynomial baseline correction and noise filtering with a symmetric 5 cm^{-1} average correction. The intensity of the peak around a Raman shift of ~1630 cm^{-1} was used as a reference of the degree of polymerization in the material, which represents the vibration of the C=C bond in the monomers and crosslinking agents in the dosimeters. The intensities of the peaks were normalized to an internal reference peak around a Raman shift of ~1800 cm^{-1}, which can be attributed to the vibration of the C=O bond present in the non-polymerized material and in the polymer or gel formed upon radiation as well. These normalized intensities are directly related to the polymerization and reaction between monomers and crosslinking agents in the material and can be used as a method to describe the chemical differences of the obtained irradiated samples (Mattea et al., 2015a). For ITABIS the vibrations of the C=C bonds at ~1630 cm^{-1} and ~1695 cm^{-1} were used to represent the MBA and ITA monomers respectively (Mattea et al., 2015b).

Finally, to prove the potential of Raman spectroscopy as an analytical tool for polymer gel dosimetry, a different experiment was carried out. Layer type phantoms were used with PAGAT manufactured with the already described methodology and stored for 24 h in a nitrogen atmosphere. Afterwards, these dosimeters were irradiated with circular collimation of 5 mm diameter for a designed dose of 20 Gy, which is close to the saturation dose value of the dosimetric material. Bidimensional distribution maps were acquired within an 80 x 80 μm^2 region as depicted in Figure, where each spectrum was processed by dedicated Matlab scripts (Matlab® version 7.11.0.584 – R2010b), and the peak area of the relevant signals was used as a descriptor for the bidimensional distribution of vinyl groups of each monomer in the studied region.

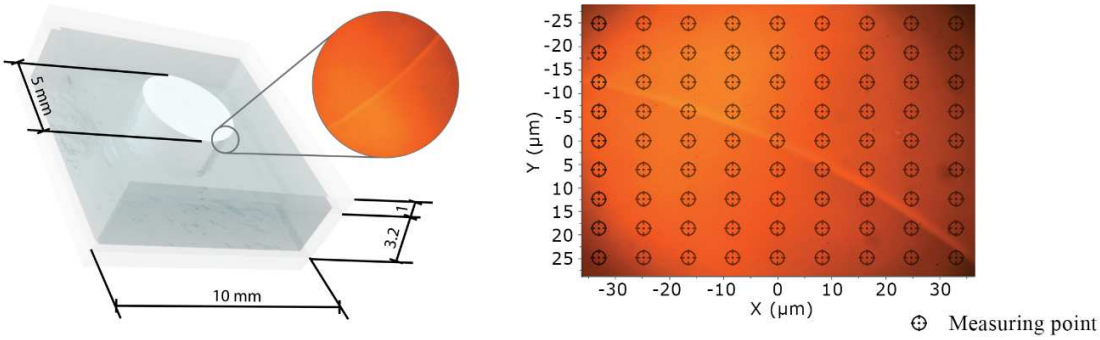

Figure 2. Scheme of the 2D Raman spectrometry analysis of layer type PAGAT dosimeters irradiated by a 5 mm diameter photon beam.

3. Results and discussion

3.1. Dose distribution simulation

The dose distribution from the MC simulation calculated in a slice of the phantom and normalized to the dose value at the center of the slice (1 x 1 mm^2 central area) with the "box" irradiation scheme is presented in Figure 3.

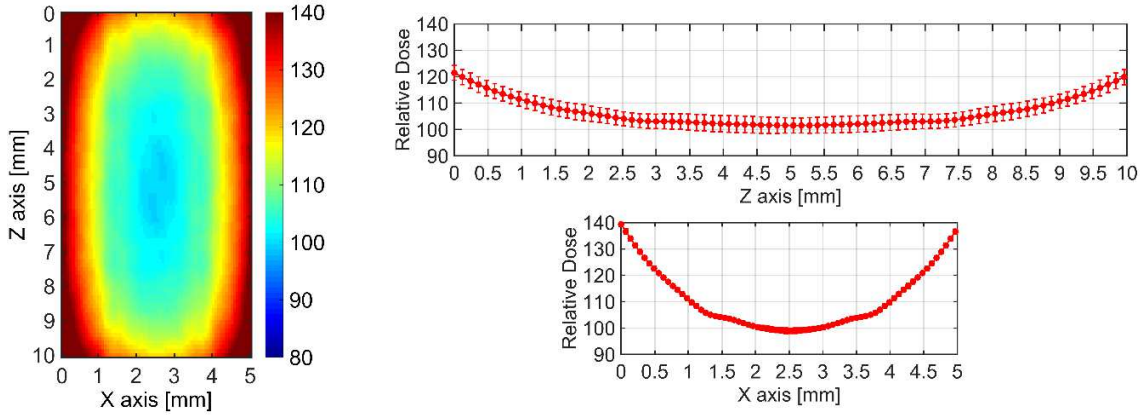

Figure 3. Relative dose distribution obtained by means of MC simulations.

MC simulations consider every type of interaction between the sample and the incident beam providing an accurate and precise dose distribution map. From the presented results it becomes clear that some regions in the samples have been exposed to a higher dose than the planned one. Moreover, the regions next to the walls of the cuvettes receive dose values up to 40% higher than the dose at the center of the sample. Although this inhomogeneity in the dose distribution could be minimized by using a different irradiation scheme, it is useful for the goal and purpose of the present study and therefore every

sample was irradiated with the presented setup. Additionally, to compare these distributions with the typical results obtained by optical methods, profiles in the Z axis at the center of the X axis and with a thickness of 3 mm, (emulating the typical thickness of the light beam used in the spectrophotometer) were calculated and presented in Figure 3. Also, profiles in the X axis at the center of the Z axis and with a thickness of 3 mm were included in Figure 3. In both profiles, the error bars are the standard deviation of the average value at that position.

Raman spectroscopy and light transmission analytical techniques evaluate a specific property in a specific plane or integrate all planes in the Z axis of the samples. Thus, precise information on the dose distribution in that axis provides key information that must be taken into account in the dose distribution maps and oxygen effect in the dosimeters.

3.2. Raman spectroscopy and light transmission dose distribution analysis

In order to assess the effects of the incorporation of oxygen during the periods before the irradiation of the samples, Raman spectroscopy and light transmission profiles were measured at different positions in the X axis of the samples. On one hand, the optical transmission images were taken, and profiles of the transmission intensities and optical densities were calculated in a selected region of interest (ROI). The results together with the optical transmission images for PAGAT are shown in Figure 4, where the optical transmission values have been normalized to the maximum value obtained in the unirradiated sample.

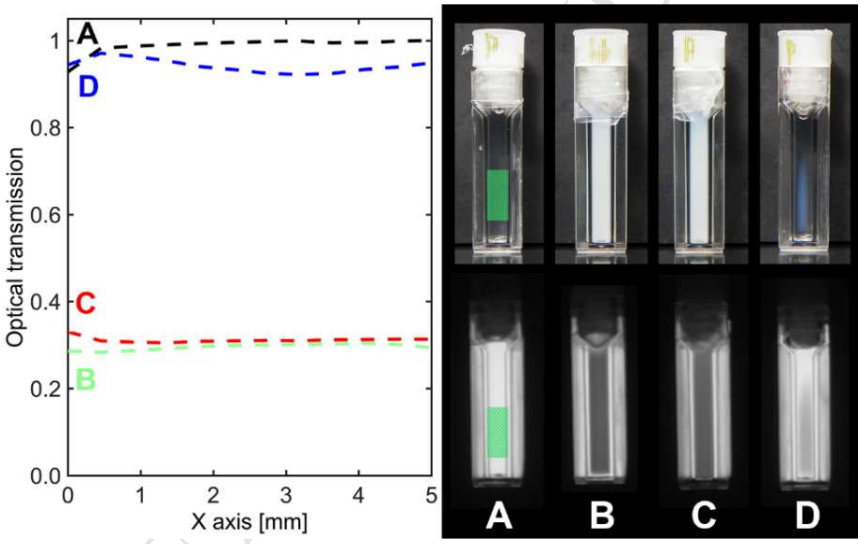

Figure 4. Visual appearance (upper row) and light transmission results (lower row) for PAGAT with different storage conditions and irradiated with a total dose of 16 Gy. (A) unirradiated dosimeter (ROI where the profiles have been analyzed is indicated in green over the sample), (B) stored in air for 2 h, (C) stored in nitrogen for 48 h and (D) stored in air for 48 h. Uncertainties in the light transmission measurements are less than 1 %.

A clear difference in the sensitive material response was observed in experiments where short periods of time were set between the manufacturing and irradiation or in experiments where samples were stored in a nitrogen atmosphere before their irradiation, compared to those which have been stored in typical conditions for 48 h before their irradiation. Light transmission values of the later, presented poor reproducibility and transmission values similar to those with no irradiation at all.

OD profiles obtained in PAGAT and NIPAM dosimeters are presented in Figure 5. A distinct effect on the proximity of the cuvette walls was present for the dosimeters irradiated after 48 h and stored in air. These dosimeters presented a maximum in the OD at the central X-Y regions of the samples and lower OD values in the rest of the cuvette. They also showed lower OD values than the ones registered by PGDs

irradiated with the same dose but stored in nitrogen. It is worthwhile mentioning that the dose deposited in the outer regions of the dosimeter is almost 40% higher than the one in the central region, therefore OD values should have the opposite trend, which is higher values in the regions next to the walls compared to the central ones. These results indicate that the polymerization undergoing within the dosimeters during their irradiation has been hindered and limited by an external factor and that this effect is more intense in the proximity of the walls of the phantoms. Nevertheless, this conclusion cannot be proved by indirect methods such as optical ones.

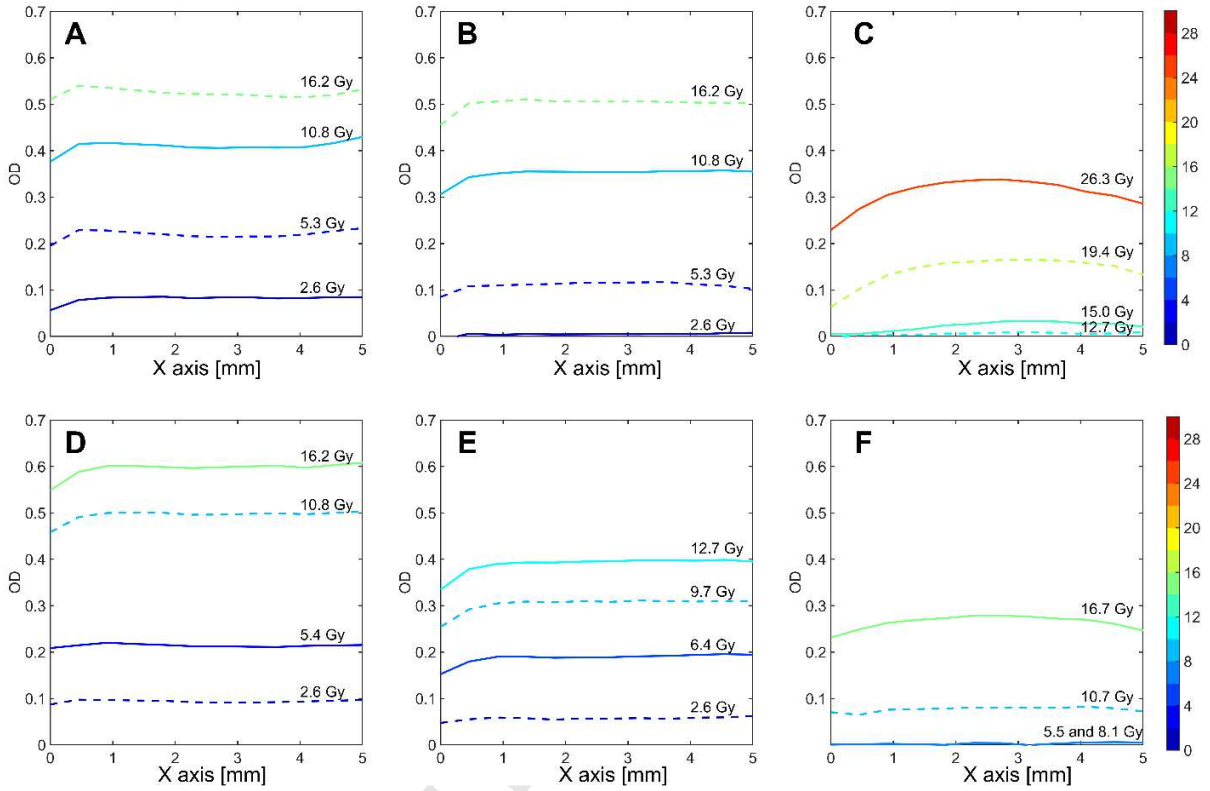

Figure 5. OD profiles for dosimeters irradiated at different doses. (A) PAGAT stored in air for 2 h, (B) PAGAT stored in nitrogen for 48 h, (C) PAGAT stored in air for 48 h, (D) NIPAM stored in air for 2 h, (E) NIPAM stored in nitrogen for 48 h, (F) NIPAM stored in air for 48 h. The color bar indicates the dose value used in each dosimeter, the uncertainties in the OD values are less than 0.035.

On the other hand, Raman spectroscopy should be able to provide useful information on the polymerization on the dosimeters. Results for PAGAT are presented in Figure 6, where a similar overall trend than the one obtained by optical methods was observed. The chemical composition of materials that have been stored in air for long periods was different compared to those where oxygen inclusion has been minimized. In this case, a lower number of vinyl bounds C=C were present within the first millimeter from the walls of the cuvettes, indicating a higher degree of polymerization in that regions in agreement with the dose distribution obtained with the MC simulations. However, after that boundary region high values of vinyl groups, that could be interpreted as a low degree of polymerization, appear indicating an inhibition of the polymerization reactions compared to the ones of the central region of the dosimeters. To aid this analysis dotted lines with the expected trend obtained from the dose profiles in the MC simulations were included in Figure 6A. In addition, the characteristic peaks of C=C vibrations practically disappeared for samples irradiated 2 h after their manufacturing and for samples irradiated 48 h after their manufacturing but stored in nitrogen, which indicates that the polymer gels have been almost saturated and that a very low amount of sensitive material remains available if doses higher than 16 Gy are used.

The spectra measured at a position of 2.14 mm from the left wall of the cuvette (2.14 of the X axis in Figure 6A) of PAGAT stored at different conditions are also depicted in Figure 6B to point out the observed differences.

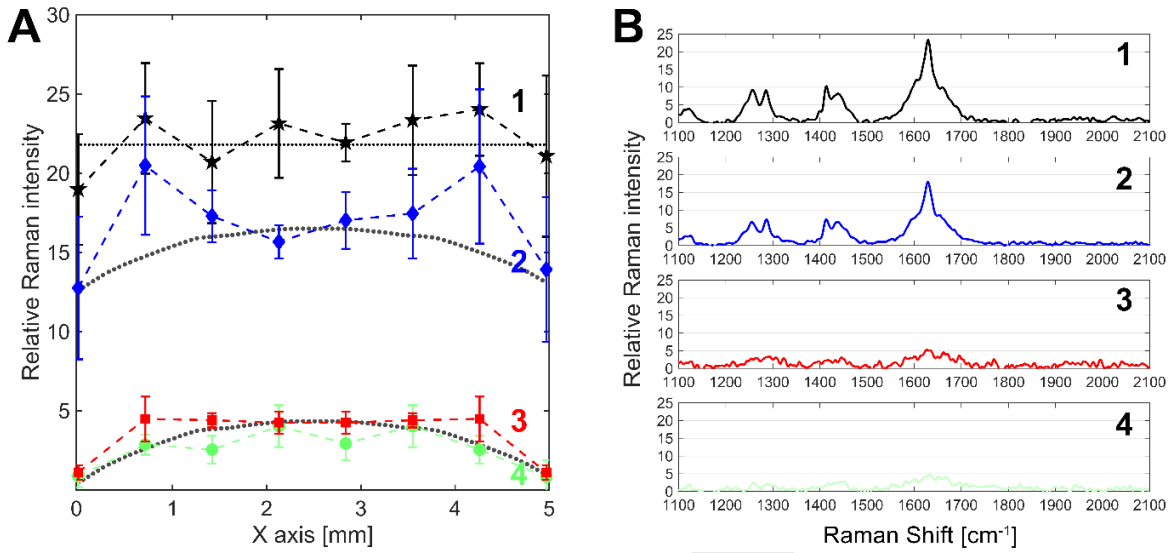

Figure 6. Raman spectroscopy results. (A) Profiles of relative intensity at different X positions in a cuvette of (1) unirradiated PAGAT, (2) irradiated PAGAT stored in air for 48 h, (3) irradiated PAGAT stored in nitrogen for 48 h and (4) irradiated PAGAT stored in air for 2 h with a total designed dose of 16 Gy. (B) Raman spectra of the same dosimeters at X position of 2.14 mm. Dashed lines are included for visualization purposes and dotted lines represent the expected trend from the MC dose distribution.

Curves 3 and 4 in Figure 6A shows that the degree of polymerization in materials, either stored in nitrogen or irradiated shortly after their manufacturing, is very similar and in agreement with the trend expected from the dose profiles obtained by the MC simulations. These results could be easily interpreted as optical artifacts or averaged by other techniques like optical methods or MRI, but thanks to Raman spectroscopy it becomes clear that the radiosensitive compounds have reacted as expected along the geometrical cross-section of the dosimeter, therefore proving that Raman spectroscopy represents an excellent tool to study non uniform oxygen inhibition in polymer gel dosimetry.

The presented results indicate that, if oxygen diffusion is avoided during the dosimeters storage, the response of the sensitive material is mostly preserved and would provide the expected dosimetry capabilities. The relative Raman intensity profiles in Figure 6 represent clear evidence that chemical differences exist within the dosimeter if oxygen diffusion happens before the irradiation of the dosimeter. The same analysis was performed for ITABIS. In this case, the PGDs were irradiated with doses ranging from 25 to 100 Gy, which are far from the saturation values of this material, as reported elsewhere (Mattea et al., 2015a), and the observed tendencies are not as evident or clear as for PAGAT. Both C=C vibration signals from the monomer and crosslinking agent have been considered in the analysis, thus the total change in the amount of reactive material in the PGD is considered and shown in Figure 7A. The results indicate that, if the atmosphere is not controlled during the ITABIS storage and the irradiation is carried out 48 h later, the regions next to the cuvette walls have more remaining sensitive material than the central part.

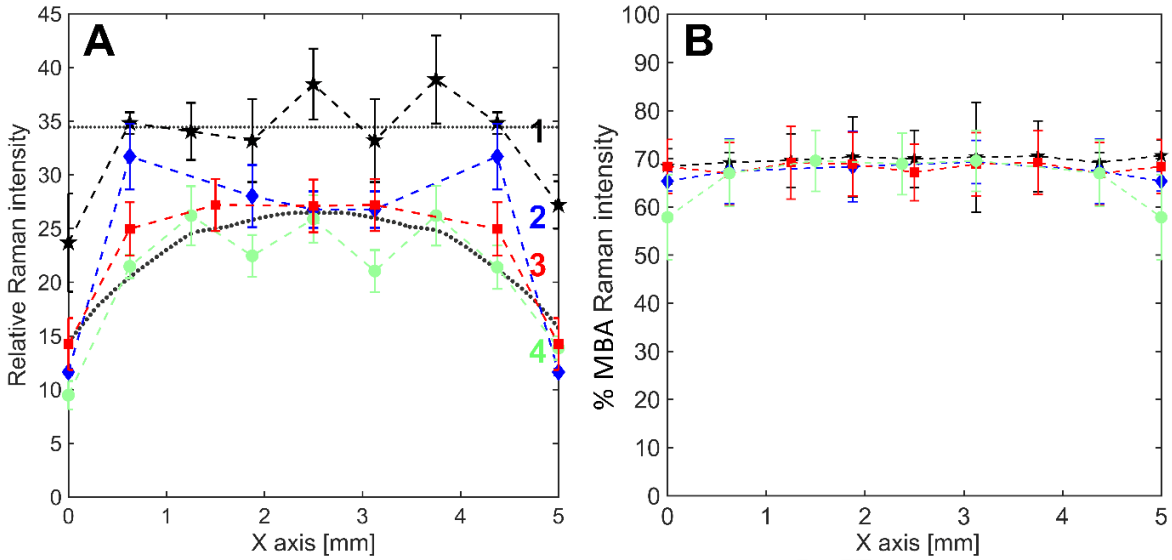

Figure 7. Raman spectroscopy results. (A) Profiles of relative intensity at different X positions in a cuvette of (1) unirradiated ITABIS dosimeter, (2) irradiated ITABIS dosimeter stored in air for 48 h, (3) irradiated ITABIS dosimeter stored in nitrogen for 48 h and (4) irradiated ITABIS dosimeter stored in air for 2 h, with a total designed dose of 105 Gy. (B) % MBA (C=C) Raman intensity for ITABIS dosimeters stored at different conditions. Dashed lines are included for visualization purposes and dotted lines represent the expected trend from the MC dose distribution.

Although the central region in all the cuvettes presented a similar degree of polymerization, values measured at positions away from the center differed between the different storage conditions. The relative intensity values for dosimeters stored in nitrogen and the ones irradiated 2 h after their preparation have very similar trends, but those stored in air for 48 h showed lower degree of polymerization than the expected one in the outer regions. However, because of the low overall degree of polymerization achieved with the dose used in this study, the errors and deviations of the method are significant, and the results are not easy to analyze. Despite of that, Raman spectroscopy was still able to measure and provide key information on the oxygen diffusion effect over the polymerization in this dosimetry material. Additionally, the percentage of the C=C Raman intensity signal of MBA (at a Raman shift of ~1630 cm^{-1}) respect to the total C=C signal (at Raman shifts of ~1630 and ~1695 cm^{-1}) was evaluated at different positions in the ITABIS dosimeters. The results presented in Figure 7B indicate that the same MBA to ITA ratio was present in every position of the dosimeters. Previous studies with PAGAT or NIPAM proved that the consumption rate of each reactive species did not show the same trend with the absorbed dose (Baldock et al., 1998); however, the ITABIS dosimetry system has the particularity of exhibiting a similar consumption among species and therefore the obtained copolymer has almost the same composition for different doses (Mattea et al. 2015). These results were independent of the storage method indicating that, even if the polymerization upon irradiation is hindered by the presence of oxygen, no specific polymerization route is preferred on each of the studied conditions.

The complete analytic results support that Raman spectroscopy is able to provide key information on the effect of oxygen diffusing through the cuvette walls during 48 h of storage, while optical methods are not able to elucidate the reason for those differences and in some cases even provided different trends. These effects were high enough to reduce the initiation and propagation steps of the polymerization reactions in the region close to those walls. In particular, the material which is located within the first millimeters from the polymeric walls presented remarkable differences in optical density and degree of polymerization than the inner part of the dosimeters. In addition, although such inhibition could be attributed to several factors, such as an antioxidant poor distribution, interaction of the sensitive materials

with the cuvette material, monomer and crosslinking agent poor distribution, described as chemical stability error sources by De Deene and Vandecasteele (De Deene & Vandecasteele, 2013), when the dosimeters were stored in nitrogen instead of air, almost no differences were observed in the response of the dosimeters. Furthermore, the results obtained with the dosimeters stored in nitrogen are really close the ones obtained with dosimeters irradiated 2 h after their manufacturing supporting the proposed hypothesis.

A bidimensional Raman spectroscopy map was also obtained for PAGAT in a micrometer region to prove the capabilities of the analytical method in the study of PGDs. A series of 81 measuring positions in a grid of 9 x 9 was used to obtain the spectra and 2D distribution presented in Figure 8. The analytical method is able to measure differences on the polymerization degree in the material with a μm resolution and detect the boundary of the irradiated area.

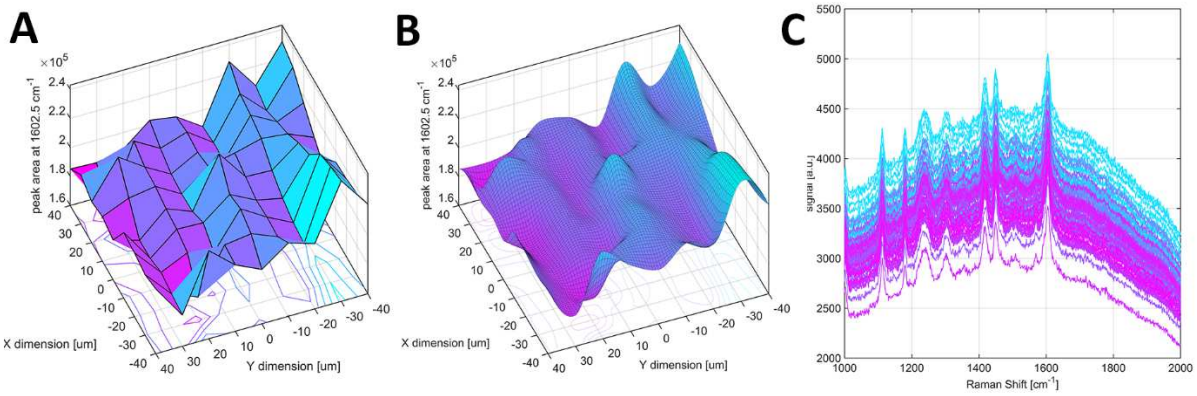

Figure 8. Raman spectroscopy 2D analysis. (A) (C=C) peak area intensity map in a selected ROI of 80x80 μm. (B) Interpolated intensity map for visualization purposes. (C) Raw Raman spectra for all the measuring points in the selected ROI.

The irradiated region by the collimation of the irradiation beam can be observed in Figures 8A and 8B, lower values in the surface indicate a lower C=C bond density, therefore a higher degree of polymerization has been achieved in that region. The distribution of vinyl groups near the irradiation boundary is not smooth and constant in the micrometer scale, polymerization is a complex process that doesn't end with the irradiation, but continues for longer periods of time, in that post-irradiation stage remaining monomers diffuses through the gelatin to react with the radicals in the polymer surface, thus producing different polymer configurations and inhomogeneities. Nevertheless, the boundary of the irradiated region is still recognizable and two different mean values can be observed at each side of the boundary.

3.3. PGD dose sensitivity and overall effect on typical analytical methods

With the aim of analyzing the limitations of commonly used analytical methods, which consider a homogeneous distribution on the delivered dose in the measured area or volume, the already described dosimeters were irradiated with different doses and the sensitivity of each material was analyzed by UV spectrophotometry and MRI. The obtained results are presented in Figures 8 and 9. All materials with storage times of 48 h in air before their irradiation and analyzed by optical methods presented a dose threshold value, which limits their practical application. For example, PAGAT needed almost 15 Gy to show an initial response compared to typical reported values below 1 Gy (Venning et al., 2005). These threshold values, which are typically associated to oxygen content (De Deene, 2004), were less pronounced on materials stored in nitrogen before their irradiation, and almost negligible for those materials irradiated 2 h after their manufacturing. The same trend was observed by means of MRI; however, the threshold values were lower compared to the ones obtained by optical methods. The sensitivity values for each material are dependent of the readout method and on the pre-irradiation

condition, and in all cases, PAGAT and NIPAM dosimeters stored for 48 h in air showed a decrease of more than 60 % in their sensitivity values.

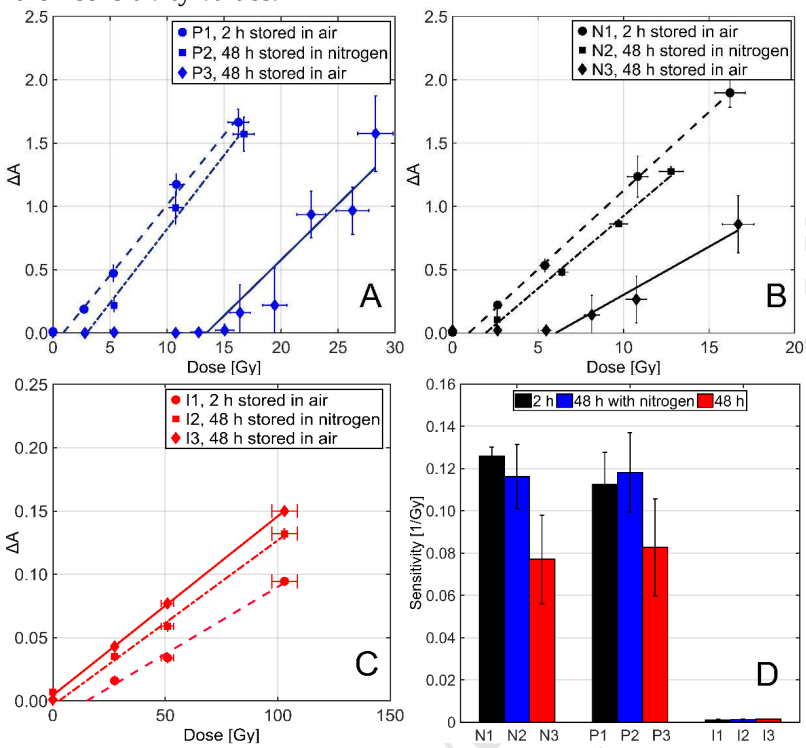

Figure 9. Dose sensitivity curves measured with light absorbance of (A) PAGAT, (B) NIPAM and (C) ITABIS with different storage conditions. (D) Dosimetry sensitivity of the different PGDs stored at different conditions.

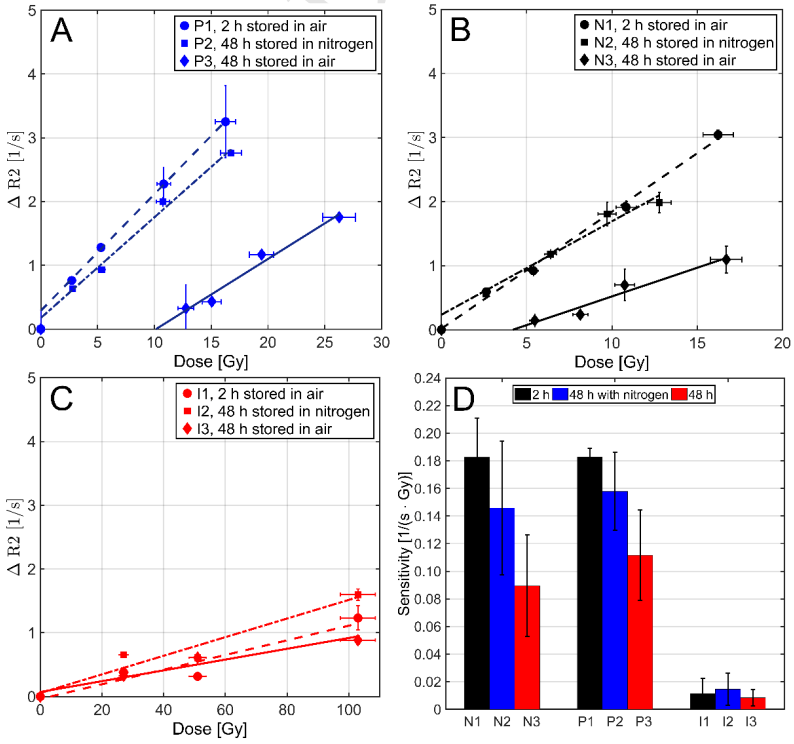

Figure 10. Dose sensitivity curves measured with MRI of (A) PAGAT, (B) NIPAM and (C) ITABIS with different storage conditions. (D) Dosimetry sensitivity of the different PGD stored at different conditions.

These results are misleading and oversimplify a complex scenario in the samples. Raman spectroscopy or optical transmission maps proved that there are inhomogeneities on the density of the formed polymer and on the polymerization degree across the sample. Methods which integrate these values and provide a unique response will provide lower responses in these cases compared to more homogeneous samples, such as the ones obtained 2 h after irradiation or the ones stored in nitrogen in the present study. What is more, in situations on which the inhomogeneities are very significant some methods will not even show a response until the signal from regions with a higher degree of polymerization compensates the low or negligible response in the other regions of the samples. Although the described effect is evident in extreme cases like the ones presented in the present study, it should still be present for methods like MRI or optical methods with low resolution in intermediate scenarios for which the polymerization becomes hindered by external effects. Therefore, the use of methods which provide direct information on the evolution of the polymerization in the samples and with high spatial resolution should be preferred if inhomogeneous or complex dose distributions are being measured.

4. Conclusions

In this study, Raman spectroscopy was used to evaluate the effect of oxygen on polymer gel dosimetry for three different materials based on acrylamide (PAGAT), N-isopropylacrylamide (NIPAM) and itaconic acid (ITABIS) and compared to optical transmission imaging results. Both methods provide information on the inhomogeneities and gradients in the response of the samples on which the inclusion of oxygen was not minimized before their irradiation. Moreover, Raman spectroscopy was the only method able to provide direct information on the degree of polymerization and nature of the formed polymer across the samples and showed that the dosimeters which were stored in nitrogen instead of air had almost the same response than those irradiated shortly after their manufacturing. Readout techniques with less resolution or those providing a unique signal for the samples showed lower responses when oxygen effects were present, and larger dose thresholds appeared on those samples with severe polymerization inhibition. Monte Carlo simulations of the dose distribution on the samples was a key element to analyze and understand the outcome of the different readout techniques. All readout methods proved that oxygen could go through typical materials that are currently being used in 3D printing of phantoms. Moreover, since complex geometries can be designed in this way, the effects in the proximity of the phantom walls become relevant and should be considered in the design of the whole dosimetry system. Different approaches could be taken to overcome these limitations, such as the use of more specific polymer with less oxygen permeability, or the use of sealed chamber for the storage of the sensitive materials before their irradiation. Finally, the results on the bidimensional mapping with Raman spectroscopy indicates that the method has enough spatial resolution to study boundary effects in polymer gel dosimetry, differences were observed in a region of 80 x 80 μm^2 showing that different degrees of polymerization were present in such a small region in PAGAT dosimeters.

Acknowledgments

This study was partially financed by CONICET by means of the Project ESPORA I - PIP 112-20130100658CO, PIP 112-0.20110101029 and SeCyT-UNC by means of DOSCOM I project and INSPIRATE I program. This project was also partially supported by Universidad de La Frontera by DIUFRO DI6008-16 project. The authors would also like to thank to Raman facilities at Laboratorio de Nanoscopía y Nanofotónica, INFIQC-CONICET/UNC, Sistema Nacional de Microscopía – MINCyT and to the Universidad Nacional (UNA) Heredia, Costa Rica for the financial support (JB-C 0612-2014) for the PhD studies of D. Chacón.

References

Adenan, M.Z., Ahmad, M., Noor, N.M., Deyhimihaghighi, N., Saion, E., 2014. Raman study of lower toxicity polymer gel for radiotherapy dosimetry. J. Phys. Conf. Ser. 546. doi:10.1088/1742-6596/546/1/012011

Baldock, C., Rintoul, L., Keevil, S.F., Pope, J.M., George, G.A., 1998. Fourier transform Raman spectroscopy of polyacrylamide gels (PAGs) for radiation dosimetry. Phys. Med. Biol. 43, 3617-3627. doi: 10.1088/0031-9155/43/12/017

Baldock, C., De Deene, Y., Doran, S., Ibbott, G., Jirasek, A., Lepage, M., McAuley, K.B., Oldham, M., Schreiner, L.J., 2010. Polymer gel dosimetry. Phys. Med. Biol. 55, R1. doi:10.1088/0031-9155/55/5/R01

Boudou, C., Troprès, I., Rousseau, J., Lamalle, L., Adam, J.F., Estève, F., Elleaume, H., 2007. Polymer gel dosimetry for synchrotron stereotactic radiotherapy and iodine dose-enhancement measurements. Phys. Med. Biol. 52, 4881–92. doi:10.1088/0031-9155/52/16/011

De Deene, Y., 2009. Review of quantitative MRI principles for gel dosimetry. J. Phys. Conf. Ser. 164, 12033. doi:10.1088/1742-6596/164/1/012033

De Deene, Y., Reynaert, N., De Wagter, C., 2001. On the accuracy of monomer/polymer gel dosimetry in the proximity of a high-dose-rate 192Ir source. Phys. Med. Biol. 46, 2801–2825. doi:10.1088/0031-9155/46/11/304

De Deene, Y., 2004. Essential characteristics of polymer gel dosimeters. J. Phys. Conf. Ser. 3, 34. doi:10.1088/1742-6596/3/1/006

De Deene, Y., Vandecasteele, J., 2013. On the reliability of 3D gel dosimetry. J. Phys. Conf. Ser. 444, 12015. doi:10.1088/1742-6596/444/1/012015

Doran, S.J., 2009. The history and principles of chemical dosimetry for 3-D radiation fields: Gels, polymers and plastics. Appl. Radiat. Isot. 67, 393–398. doi:10.1016/j.apradiso.2008.06.026

Elter, A., Dorsch, S., Mann, P., Runz, A., Johnen, W., Karger, C.P., 2019. Compatibility of 3D printing materials and printing techniques with PAGAT gel dosimetry. Phys Med Biol 64, 04NT02.

Fong, P.M., Keil, D.C., Does, M.D., Gore, J.C., 2001. Polymer gels for magnetic resonance imaging of radiation dose distributions at normal room atmosphere. Phys Med Biol 46, 3105–3113.

Gastaldo, J., Boudou, C., Lamalle, L., Troprès, I., Corde, S., Sollier, A., Rucka, G., Elleaume, H., 2008. Normoxic polyacrylamide gel doped with iodine: Response versus X-ray energy. Eur. J. Radiol. 68, 118–120. doi:10.1016/j.ejrad.2008.04.053

Hill, B., Venning, A.J., Baldock, C., 2005. A preliminary study of the novel application of normoxic polymer gel dosimeters for the measurement of CTDI on diagnostic x-ray CT scanners. Med. Phys. 32, 1589–1597. doi:10.1118/1.1925181

Huang, Y.R., Hsieh, L.L., Chang, Y.J., Wang, T.H., Hsieh, B.T., 2013. Characterization of the chemical stability of irradiated N-isopropylacrylamide gel dosimeter. Radiat. Phys. Chem. 89, 76-82. doi: 10.1016/j.radphyschem.2013.03.047.

IAEA, 2000. Absorbed dose determination in external beam radiotherapy: An international code of practice for dosimetry on standards of absorbed dose to water Technical Report Series 398. Vienna: International Atomic Energy Agency.

Ibbott, G.S., Maryanski, M.J., Eastman, P., Holcomb, S.D., Zhang, Y., Avison, R.G., Sanders, M., Gore, J.C., 1997. Three-dimensional visualization and measurement of conformal dose distributions using magnetic resonance imaging of bang polymer gel dosimeters. Int. J. Radiat. Oncol. Biol. Phys. 38, 1097–1103. doi:10.1016/S0360-3016(97)00146-6

Jirasek, A., Hilts, M., Shaw, C., Baxter, P., 2006. Investigation of tetrakis hydroxymethyl phosphonium chloride as an antioxidant for use in x-ray computed tomography polyacrylamide gel dosimetry. Phys. Med. Biol. 51, 1891. doi:10.1088/0031-9155/51/7/018

Jirasek, A., 2010. Alternative imaging modalities for polymer gel dosimetry. Journal of Physics: Conference Series. 250, 102070. doi: 10.1088/1742-6596/250/1/012070

Lepage, M., 2006. Magnetic resonance in polymer gel dosimetry: techniques and optimization. Journal of Physics: Conference Series. 56, 86-94. doi: 10.1088/1742-6596/56/1/008

Maryanski, M.J., Gore, J.C., Kennan, R.P., Schulz, R.J., 1993. NMR relaxation enhancement in gels

polymerized and cross-linked by ionizing radiation: A new approach to 3D dosimetry by MRI. Magn. Reson. Imaging 11, 253–258. doi:10.1016/0730-725X(93)90030-H

Maryanski, M.J., Schulz, R.J., Ibbott G.S., Gatenby J.C., Xie J., Horton D., Gore, J.C., 1994. Magnetic resonance imaging of radiation dose distributions using a polymer-gel dosimeter. Phys. Med. Biol. 39, 1437-1455. doi: 10.1088/0031-9155/39/9/010

Mattea, F., Chacón, D., Vedelago, J., Valente, M., Strumia, M.C., 2015a. Polymer gel dosimeter based on itaconic acid. Appl. Radiat. Isot. 105, 98–104. doi:10.1016/j.apradiso.2015.07.042

Mattea, F., Romero, M., Vedelago, J., Quiroga, A., Valente, M., Strumia, M.C., 2015b. Molecular structure effects on the post irradiation diffusion in polymer gel dosimeters. Appl. Radiat. Isot. 100, 101–107. doi:10.1016/j.apradiso.2015.03.007

Mesbahi, A., Jafarzadeh, V., Gharehaghaji, N., 2012. Optical and NMR dose response of N-isopropylacrylamide normoxic polymer gel for radiation therapy dosimetry. Reports Pract. Oncol. Radiother. 17, 146–150. doi:10.1016/j.rpor.2012.03.009

Rabaeh, K.A., Basfar, A.A., Almousa, A.A., Devic, S., Moftah, B., 2017. New normoxic N-(Hydroxymethyl)acrylamide based polymer gel for 3D dosimetry in radiation therapy. Phys. Medica 33, 121–126. doi:10.1016/j.ejmp.2016.12.019

Rintoul, L., Lepage, M., Baldock, C., 2003. Radiation dose distribution in polymer gels by Raman spectroscopy. Appl. Spectrosc. 57, 51–57. doi:10.1366/000370203321165205

Salvat, F., Fernández-Varea, J.M., Sempau, J., 2006. PENELOPE-2006: A Code System for Monte Carlo Simulation of Electron and Photon Transport, in: Workshop Proceedings. National Energy Agency, Barcelona.

Schreiner, L.J., 2004. Review of Fricke gel dosimeters. J. Phys. Conf. Ser. 3, 9–21. doi:10.1088/1742-6596/3/1/003

Sedaghat, M., Bujold, R., Lepage, M., 2012. Preliminary studies on the role and reactions of tetrakis(hydroxymethyl)phosphonium chloride in polyacrylamide gel dosimeters. Phys. Med. Biol. 57, 5981–5994. doi:10.1088/0031-9155/57/19/5981

Sedaghat, M., Bujold, R., Lepage, M., 2011. Investigating potential physicochemical errors in polymer gel dosimeters. Phys. Med. Biol. 56, 6083–6107. doi:10.1088/0031-9155/56/18/019

Senden, R.J., De Jean, P., McAuley, K.B., Schreiner, L.J., 2006. Polymer gel dosimeters with reduced toxicity: a preliminary investigation of the NMR and optical dose-response using different monomers. Phys. Med. Biol. 51, 3301–14. doi:10.1088/0031-9155/51/14/001

Titus, D., Samuel, E.J.J., Mohana Roopan, S., 2016. Current scenario of biomedical aspect of metal-based nanoparticles on gel dosimetry. Appl. Microbiol. Biotechnol. 100, 4803–4816. doi:10.1007/s00253-016-7489-5

Valente, M., Grana, D., Malano, F., Perez, P., Quintana, C., Tirao, G., Vedelago, J., 2016. Development and characterization of a microCT facility. IEEE Lat. Am. Trans. 14, 3967–3973. doi:10.1109/TLA.2016.7785920

Vedelago, J., Obando, D.C., Malano, F., Conejeros, R., Figueroa, R., Garcia, D., González, G., Romero, M., Santibañez, M., Strumia, M.C., Velásquez, J., Mattea, F., Valente, M., 2016. Fricke and polymer gel 2D dosimetry validation using Monte Carlo simulation. Radiat. Meas. 91, 54–64. doi:10.1016/j.radmeas.2016.05.003

Venning, A.J., Hill, B., Brindha, S., Healy, B.J., Baldock, C., 2005. Investigation of the PAGAT polymer gel dosimeter using magnetic resonance imaging. Phys. Med. Biol. 50, 3875. doi:10.1088/0031-9155/50/16/015

Highlights

- Raman spectroscopy was used to study oxygen effects in three polymer gel dosimeters.
- Raman methods can measure different polymerization degrees in the micrometer scale.
- Storing dosimeters in nitrogen is a simple alternative if PMMA phantoms are used.
- PAGAT, NIPAM and itaconic acid dosimetry can be analyzed by Raman spectroscopy.